Hippocampus chronic deep brain stimulation induces reversible transcript changes in a macaque model of mesial temporal lobe epilepsy

Ning Chen[1,2], Jian-Guo Zhang[1,2], Chun-Lei Han[1,2], Fan-Gang Meng[2,3,4]

[1]Department of Neurosurgery, Beijing Tiantan Hospital, Capital Medical University, Beijing 100070, China;
[2]Beijing Key Laboratory of Neuromodulation, Beijing Municipal Science and Technology Commission, Beijing 100070, China;
[3]Beijing Neurosurgical Institute, Capital Medical University, Beijing 100070, China;
[4]Chinese Institute for Brain Research, Beijing 102206, China.

Abstract

Background: Deep brain stimulation (DBS) has seizure-suppressing effects but the molecular mechanisms underlying its therapeutic action remain unclear. This study aimed to systematically elucidate the mechanisms underlying DBS-induced seizure suppression at a molecular level.

Methods: We established a macaque model of mesial temporal lobe epilepsy (mTLE), and continuous high-frequency hippocampus DBS (hip-DBS) was applied for 3 months. The effects of hip-DBS on hippocampus gene expression were examined using high-throughput microarray analysis followed by bioinformatics analysis. Moreover, the microarray results were validated using quantitative real-time polymerase chain reaction (qRT-PCR) and Western blot analyses.

Results: The results showed that chronic hip-DBS modulated the hippocampal gene expression. We identified 4119 differentially expressed genes and assigned these genes to 16 model profiles. Series test of cluster analysis showed that profiles 5, 3, and 2 were the predominant expression profiles. Moreover, profile 5 was mainly involved in focal adhesion and extracellular matrix-receptor interaction pathway. Nine dysregulated genes (*Arhgap5*, *Col1a2*, *Itgb1*, *Pik3r1*, *Lama4*, *Fn1*, *Col3a1*, *Itga9*, and *Shc4*) and three genes (*Col1a2*, *Itgb1*, and *Flna*) in these two pathways were further validated by qRT-PCR and Western blot analyses, respectively, which showed a concordance.

Conclusion: Our findings suggest that hip-DBS could markedly reverse mTLE-induced abnormal gene expression. Findings from this study establish the basis for further investigation of the underlying regulatory mechanisms of DBS for mTLE.

Keywords: Deep brain stimulation; Gene expression profile; Hippocampus; Temporal lobe epilepsy

Introduction

Epilepsy is a common neurological disorder characterized by recurrent, unprovoked seizures, which has a prevalence of 0.5% to 1% worldwide. Mesial temporal lobe epilepsy (mTLE) is the most common epilepsy syndrome and is often associated with pharmacoresistance. About 30% of patients have pharmacologically resistant epilepsy.[1,2] Hippocampus deep brain stimulation (hip-DBS) is increasingly being used in the treatment of refractory temporal lobe epilepsy and showed a good therapeutic effect.[3,4] While these studies suggest hip-DBS to be effective in pharmacoresistant mTLE, the mechanisms underlying the therapeutic effects at the cellular and molecular levels remain poorly understood.

Access this article online

Quick Response Code:

Website: www.cmj.org

DOI: 10.1097/CM9.0000000000001644

A number of molecular studies on the mechanism of mTLE hip-DBS have been reported recently.[5-8] It has been shown that hip-DBS could induce anti-apoptotic and anti-inflammatory effects in epileptic rats through countering the increase of caspase 3 and interleukin-6 levels in the hippocampus.[9] In addition, low-frequency hip-DBS increased the expression of the gamma-aminobutyric acid type B receptors[10,11] and high-frequency hip-DBS increased gamma-aminobutyric acid levels at the parahippocampal cortex, with a significant increase in cell count when compared with the patients in mTLE group.[12] Moreover, glucose utilization could be inhibited by hip-DBS in the hippocampus of healthy rats.[13] In our

Correspondence to: Dr. Chun-Lei Han, Department of Neurosurgery, Beijing Tiantan Hospital, Capital Medical University, Beijing 100070, China
E-Mail: hanchunlei622@163.com
Prof. Fan-Gang Meng, Beijing Neurosurgical Institute, Capital Medical University, Beijing 100070, China
E-Mail: fgmeng@ccmu.edu.cn

Chinese Medical Journal 2021;134(15)
Received: 23-12-2020 **Edited by:** Yan-Jie Yin and Xiu-Yuan Hao

previous work, we have successfully established a macaque model of mTLE[14] and found that hip-DBS attenuated changes in apoptosis-related proteins and robustly decreased neuronal loss.[15]

However, the specific molecular targets of hip-DBS remain unknown. In the present study, we performed high-throughput microarray assays and analyzed the role of hip-DBS on gene expression in an mTLE macaque model. We identified genes that were differentially regulated at the transcription level and the alteration profiles of genes from the hippocampus.

Methods

Ethical approval

The care and handling of animals were conducted in compliance with the Chinese Animal Welfare Act, the Guidance for Animal Experimentation of Capital Medical University, and Beijing guidelines for the care and use of laboratory animals. The study was approved by the Ethics Committee of Beijing Neurosurgical Institute, Capital Medical University (No. 20120619). Efforts were made to minimize the number of animals used and their suffering.

Animals

Nine male macaques from Laboratory Animal Center, Academy of Military Medical Science, were divided into three groups: the control group ($n = 3$; macaques received right intra-hippocampal saline injections without implantation of electrodes into the hippocampus), the kainic acid (KA) group ($n = 3$; macaques received right intra-hippocampal KA injections without implantation of electrodes into the hippocampus), and the KA + hip-DBS group ($n = 3$; macaques received right intra-hippocampal KA injections after undergoing implantation of electrodes into the ipsilateral hippocampus and DBS was applied as described below).

Epilepsy model and hip-DBS treatment

Animal experiments were performed according to previously described techniques.[14,15] Briefly, the macaques were anesthetized with ketamine hydrochloride (10.00 mg/kg, intramuscular; Shuanghe Pharmaceutical, Beijing, China). Electrodes were implanted in the DBS group within the right hippocampus (8.10 mm posterior to bregma, 12.00 mm lateral from midline, and 35.30 mm ventral to bregma). The placement of electrode at the correct position was confirmed by magnetic resonance imaging as described previously.[15] All macaques were recovered from the surgery for 7 days. After 7 days, a total of 7 μL KA (2 μg/μL; Sigma Chemical Co., St. Louis, MO, USA) was stereotaxically injected into the right hippocampus (8.55 mm posterior to bregma, 12.00 mm lateral from midline, and 35.30 mm ventral to bregma). The macaques that received intra-hippocampus saline injections were used as sham-operated controls. The macaques received continuous electrical stimulation of the hippocampus immediately following KA administration. The electrical stimulation voltage was 1.5 V, the wave width was 450 μs, and the frequency was 130 Hz. Hip-DBS was applied continuously for 3 months, and video recordings were used to monitor macaques over 3 months to detect spontaneous seizures.

Sample preparation and microarray analysis

After 3 months' DBS, the experimental macaques were anesthetized and fixed on an operating table, and ipsilateral hippocampus resection was performed. Each resected sample was cut along the horizontal axis into several parts and immediately placed in liquid nitrogen for subsequent analyses. For microarray analysis, total RNA was extracted from six of the nine individual samples using the miRNeasy Mini Kit (QIAGEN, Hilden, Germany) according to the manufacturer's protocol. RNA was amplified and transcribed into cRNA by utilizing a random priming method, and cDNA was labeled and hybridized to the Affymetrix GeneChip Rhesus Macaque Genome Array (Affymetrix, Santa Clara, CA, USA). Microarray analysis was performed and repeated three times. The arrays were scanned by GeneChip Scanner 3000 7G (Affymetrix, Santa Clara, CA, USA), and the acquired array images were analyzed by Affymetrix GeneChip Operating Software (Affymetrix, Santa Clara, CA, USA).

Bioinformatic analysis

We applied fold-change filtering (fold change ≥2) to filter the differentially expressed genes in the control and experiment groups because there were two samples in each group during the microarray analysis process. Any two groups of the three sets of data were compared, and the union of the three sets of differential expression genes was calculated.

The series test of cluster (STC) algorithm of gene expression dynamics was used to profile the gene expression series (control, KA, and KA + hip-DBS groups) and to identify the most probable set of clusters. This method explicitly considered the dynamic nature of the temporal gene expression profiles during clustering and identified the number of distinct clusters. We selected differential expression genes at a logical sequence according to random variance model corrective one-way analysis of variance (ANOVA). In accordance with different signal density change tendencies of genes under different situations, we identified a set of unique model expression tendencies. The raw expression values were converted into $\log_2$ ratio. Using a strategy for clustering short time-series gene expression data, we defined some unique profiles. The expression model profiles were related to the actual or the expected number of genes assigned to each model profile. Significant profiles had a higher probability than expected by Fisher exact and multiple comparison tests.[16]

Gene ontology (GO) and pathway analysis were applied to analyze the main function of the differential expression genes.[17] Specifically, two-side Fisher exact and χ^2 tests were used to classify the GO category and to select the significant pathway, and the false discovery rate (FDR) was calculated to correct the P value, the smaller the FDR, and $P < 0.050$ was considered to be significant.[18] The Path-Net was the interaction net of the significant pathways of the

differential expression genes, and it was built according to the interaction among pathways of the Kyoto Encyclopedia of Genes and Genomes (KEGG) database to find the interaction among the significant pathways directly and systemically. It could summarize the pathway interaction of differential expression genes under diseases and found out the reason why certain pathway was activated.[19]

Gene-gene interaction network was constructed based on the data of differentially expressed genes. Using java that allows users to build and analyze molecular networks, network maps were constructed. The considered evidence was the source of the interaction database from KEGG. Networks were stored and presented as graphs, where nodes were mainly genes (protein, compound, etc) and edges represented relation types between the nodes, for example, activation or phosphorylation. The graph nature of networks raised our interest to investigate them with powerful tools implemented in R.

To investigate the global network, we computationally identified the most important nodes. To this end, we turned to the connectivity (also known as degree) defined as the sum of connection strengths with the other network genes. In gene networks, the connectivity measured how correlated a gene was with all other network genes. For a gene in the network, the number of source genes of a gene was called the indegree of the gene and the number of target genes of a gene was its outdegree. The character of genes was described by betweenness centrality measures reflecting the importance of a node in a graph relative to the other nodes. For a graph G: (V, E) with n vertices, the relative betweenness centrality was defined by: $C_B'(v) = \frac{2}{n^2-3n+2} \sum_{\substack{s \neq v \neq t \in V \\ s \neq t}} \frac{\sigma_{st}(v)}{\sigma_{st}}$ where σ_{st} was the number of shortest paths from s to t, and $\sigma_{st}(v)$ was the number of shortest paths from s to t that passed through a vertex v.[20-24]

In the network analysis, the degree centrality was one of the simplest and most important measures of the centrality of a gene and its relative importance within a network. Degree centrality was defined as the number of links that one node had to all of the other nodes.[25] Moreover, in studying some properties of the networks, k-cores in graph theory were introduced as a method of simplifying the analysis of graph topologies. A k-core of a network was a sub-network in which all nodes were connected to at least k other genes in the sub-network. A k-core of a protein-protein interaction network usually contained cohesive groups of proteins

Quantitative real-time polymerase chain reaction (qRT-PCR)

Nine genes, which were included in both profile 5 and belonged to extracellular matrix (ECM)-receptor interaction and focal adhesion pathway, were selected. Total RNA was extracted from the hippocampus using a standard TRIzol procedure from each tissue sample (Cat#CW0581, CWbio., Beijing, China). Total RNA was purified (Cat#CW2090, CWbio., Beijing, China), and cDNA synthesis was performed using a HiFi-MMLV cDNA reagent kit (Cat#CW0744, CWbio., Beijing, China). Equivalent amounts of cDNA were used for real-time PCR in a 20-μL reaction volume containing 10 μL of 2×UltraSYBR Mixture (Cat#CW0956, CWbio., Beijing, China) and 2 μL of specific primer pairs. The qRT-PCR reaction was incubated at 95°C for 15 min, followed by 45 cycles of 95°C for 10 s, 55°C for 20 s, and 72°C for 20 s, and a melt curve analysis. Each qRT-PCR was conducted in triplicate performed in a CFX96 Touch (Bio-Rad, CA, USA). Sequences of each primer are listed in Supplementary Table S1, http://links.lww.com/CM9/A686. The real-time value for each sample was averaged and compared using the cycle threshold method, where the amount of target RNA ($2^{-\Delta\Delta CT}$) was normalized to the endogenous monkey actin reference (ΔCT).

Western blotting analysis

Hippocampal tissues were homogenized in lysis buffer containing protease inhibitors and phosphatase inhibitor cocktail (p0013B, Beyotime Biotechnology, Shanghai, China). Equal amounts of protein (50 μg per line) in sample buffer were denatured at 95 °C for 5 min and separated on 10% acrylamide gel. The proteins from the gel were transferred to a nitrocellulose membrane. The membranes were incubated in 3% non-fat milk in Tris buffer for 30 min and then incubated overnight with primary antibodies against: Col1a2 (1:500; Abcam/ab96723, Cambridge, MA, USA), Flna (1:100; Abcam/ab76289, Cambridge, MA, USA), Itgb1 (1:500; Abcam/ab179471, Cambridge, MA, USA) and glyceraldehyde-3-phosphate dehydrogenase (GAPDH) (1:4000; Abcam/ab181602, Cambridge, MA, USA). Subsequently, the membranes were incubated with secondary anti-rabbit (1:5000; Santa/Sc-2004, Santa Cruz, CA, USA), followed by chemiluminescent detection by enhanced chemiluminescence (Thermo/34080). The density of the bands on the membrane was scanned and analyzed with LabWorks Image Analysis Software (UVP, Inc., San Gabriel, CA, USA).

Statistical analysis

Data were analyzed using GraphPad Prism 5 statistical software (GraphPad Software Inc., San Diego, CA, USA). qRT-PCR and Western blot data were compared by ANOVA post-Dunnett multiple comparison test. A P value < 0.050 was considered to be statistically significant. Data in all figures were expressed as mean ± standard error of the mean.

Results

Screening of differentially expressed genes associated with hip-DBS

As reported by our studies previously, hip-DBS inhibited the spontaneous recurrent seizures in epileptic monkeys.[15] To identify differentially expressed genes, we performed fold-change filtering between control, KA, and KA + hip-DBS groups (fold change >2.0). We found that there were 1597 differentially expressed genes between the control and KA groups, 1062 differentially expressed genes between KA and KA + hip-DBS groups, and 1460 differentially expressed genes between KA + hip-DBS and control groups. From these three data sets, we found a total

of 4119 differential expression genes [Supplementary Material 1, http://links.lww.com/CM9/A680].

STC analysis

To further narrow down the target genes which harbor more significance among the discovered 4119 genes, the STC analysis was performed using Time-series Expression Miner (STEM) software (http://www.cs.cmu.edu/jernst/stem/). After the STC analysis, these differential genes were divided into 16 types of expression profiles according to the alignment of the control, KA, and KA + hip-DBS groups [Figure 1]. As shown in Figure 1A, each profile contains a cluster of multiple genes that have similar expression patterns among the three groups. Among the 16 patterns, three expression patterns including profiles 5, 3, and 2 showed statistical significance ($P < 0.001$). Profile 5 was composed of genes that elevated in KA group and then gradually decreased in KA + hip-DBS group. Profile 3 contained genes that were elevated in KA group and then remained unchanged in expression in KA + hip-DBS group. Profile 2 contained genes that showed gradually elevated expression in KA group and then further increased in KA + hip-DBS group [Figure 1B–D]. All genes of profiles 5, 3, and 2 are listed in Supplementary Material 2, http://links.lww.com/CM9/A681.

GO and pathway analysis of the differential genes associated with KA and hip-DBS

The comprehensive GO analysis of differentially expressed genes was performed to gain deeper insight into the main functions related to KA and hip-DBS. After filtering using the significant criterion of $P < 0.050$, we reached 102 significant GO terms that fell in the range of key functional classifications [see Supplementary Material 3, http://links.lww.com/CM9/A682]. The first 20 GO terms that exhibited significant differences among the three groups are shown in Figure 2A.

Using the Database for Annotation, Visualization, and Integrated Discovery software based on the KEGG pathway map, we further investigated the key pathways related to these genes. The significant pathway categories ($P < 0.050$) of all significant differential genes are displayed in Figure 2B and Supplementary Material 4, http://links.lww.com/CM9/A683. Our analysis yielded 13 significant pathways, including calcium signaling pathway ($P < 0.001$), ECM-receptor interaction ($P < 0.010$), focal adhesion ($P < 0.010$), mitogen-activated protein kinase (MAPK) signaling pathway ($P < 0.050$), bacterial invasion of epithelial cells ($P < 0.050$), sphingolipid metabolism ($P < 0.050$), hypertrophic cardiomyopathy ($P < 0.050$), amino sugar ($P < 0.050$), nucleotide sugar metabolism ($P < 0.050$), type II diabetes mellitus ($P < 0.050$), pathways in cancer ($P < 0.050$), axon guidance ($P < 0.050$), erythroblastic leukemia viral oncogene homolog signaling pathway ($P < 0.050$), and biotin metabolism ($P < 0.050$). Interestingly, except the gene *met*, all the genes of ECM-receptor interaction and focal adhesion were involved in profile 5 [Table 1 and Supplementary Material 2, http://links.lww.com/CM9/A681].

To identify the interaction directly and systemically among the pathways, the interaction network of the significant pathways was built according to the KEGG database. As shown in Figure 3, the key pathway interaction was mainly involved in MAPK signaling pathway, pathways in cancer,

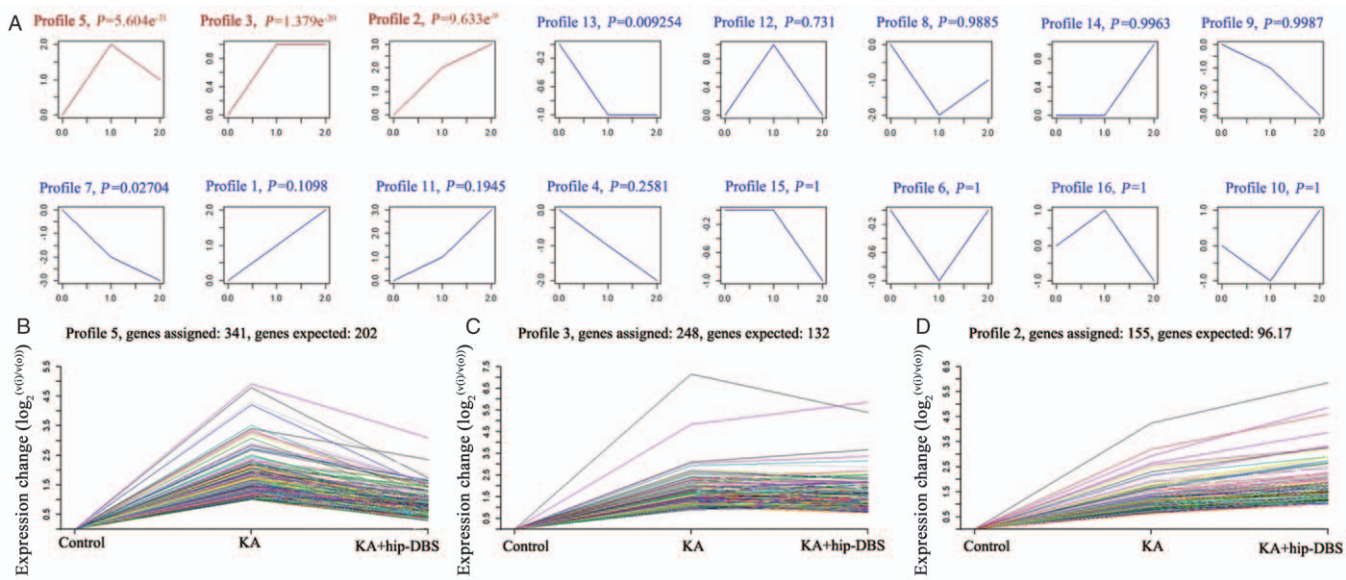

Figure 1: STC analysis for differential genes among the control, KA, and KA + hip-DBS groups. (A) Sixteen model profiles were used to summarize the expression patterns of differential genes. Each box represented a model expression profile. The model profile number and the *P* value were presented on the top of the profile box. The horizontal axis (0.0, 1.0, and 2.0) was for the three group points (control, KA, and KA + hip-DBS, respectively), and the vertical axis showed the gene expression levels after log-normalized transformation. The expression patterns with significant differences ($P < 0.001$) were displayed in red. (B–D) Three expression patterns with a significant difference were displayed. The upper row in the profile figure was the model profile ID number, the number of the genes assigned and expected to the profile. The horizontal axis represented the three group points (control, KA, and KA + hip-DBS), and the vertical axis showed the gene expression levels after log-normalized transformation. The curves show individual gene expression profiles, and each curve represents an individual gene. hip-DBS: Hippocampus-deep brain stimulation; KA: Kainic acid.

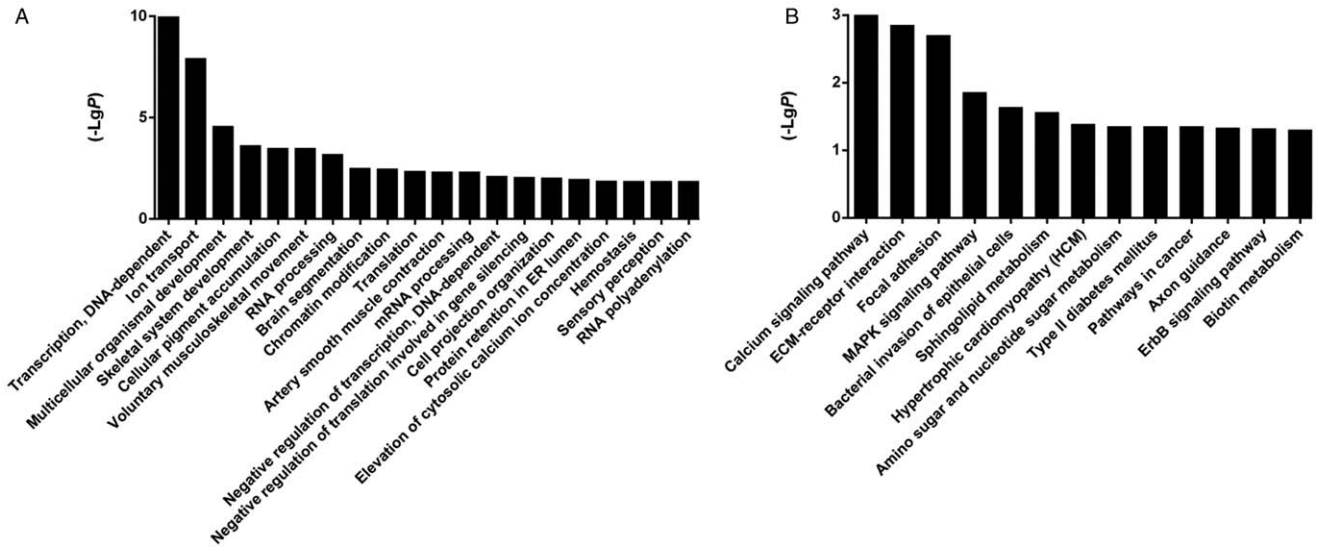

Figure 2: GO and pathway analysis. The first 20 GO IDs (A) and all of the pathways (B) that exhibited significant differences among the three groups (control, KA, and KA + hip-DBS) were listed. The horizontal axis is for the GO or pathway ID, and the vertical axis shows the significance of difference after log-normalized transformation. GO: Gene ontology; hip-DBS: Hippocampus-deep brain stimulation; KA: Kainic acid.

Table 1: The differentially expressed genes of ECM-receptor interaction and focal adhesion pathway.

Pathway	Gene name	*P*
ECM-receptor interaction	*Cd44*	0.001
ECM-receptor interaction	*Col6a1*	0.001
ECM-receptor interaction	*Col1a2*	0.001
ECM-receptor interaction	*Itgb1*	0.001
ECM-receptor interaction	*Col3a1*	0.001
ECM–receptor interaction	*Itga9*	0.001
Focal adhesion	*Col6a1*	0.002
Focal adhesion	*Col1a2*	0.002
Focal adhesion	*Pik3r1*	0.002
Focal adhesion	*Itgb1*	0.002
Focal adhesion	*Arhgap5*	0.002
Focal adhesion	*Shc4*	0.002
Focal adhesion	*Met*	0.002
Focal adhesion	*Col3a1*	0.002
Focal adhesion	*Itga9*	0.002

ECM: Extracellular matrix.

ECM-receptor interaction, and focal adhesion. As shown in Figure 3, pathways in cancer were in the upstream position, which were related to ECM-receptor interaction, focal adhesion, erythroblastic leukemia viral oncogene homolog signaling pathway, and calcium signaling pathway. Finally, all pathways indicated to MAPK signaling pathway.

Signal-net analysis of differentially expressed genes related to KA and hip-DBS

To investigate the key genes involved in KA and hip-DBS and their interaction, regulatory network maps were constructed. Approximately 102 genes were included in the signet. Of the differentially expressed genes, *Hsp90aa1* (degree = 27), *Srsf1* (degree = 25), *Ddx17* (degree = 22), *Pcbp2* (degree = 21), *Hnrnpd* (degree = 21), and *Myl6* (degree = 18) were the most significantly altered genes according to the degree size [Figure 4 and Supplementary Material 5, http://links.lww.com/CM9/A684].

Internal molecule network targeted by KA and hip-DBS

As shown in Figure 5 of the integrity co-expression network, Loc100424862 (degree = 24), Eed (degree = 23), Twist1 (degree = 20), Sart3 (degree = 20), and Clk4 (degree = 20) were the core nodes in the cortex network [Figure 5 and Supplementary Material 6, http://links.lww.com/CM9/A685].

Validation of the microarray data using qRT-PCR

To validate the microarray analysis findings, the expression level of nine genes of focal adhesion pathway in Table 1 and also of Profile 5 were analyzed using qRT-PCR. The results showed that six genes (*Arhgap5*, *Col1a2*, *Itgb1*, *Pik3r1*, *Lama4*, and *Fn1*) out of nine genes were consistent with the microarray, while three genes (*Col3a1*, *Itga9*, and *Shc4*) were not in line with the expected trend. However, only one gene (*Col1a2*) showed significant differences among the three groups (control *vs.* KA: $P < 0.001$; KA *vs.* KA + hip-DBS: $P < 0.001$; control *vs.* KA + hip-DBS: ns) [Figure 6].

Validation of the microarray data using Western blot

To further verify the microarray results, three proteins (Col1a2, Flna, and Itgb1) of the focal adhesion pathway were analyzed using Western blot. Expression of all the three proteins was increased following KA injection in the mTLE group compared with the control group (Col1a2, Flna: $P < 0.001$, Itgb1: $P < 0.010$). Importantly, hip-DBS in mTLE model (mTLE + hip-DBS group) reversed the

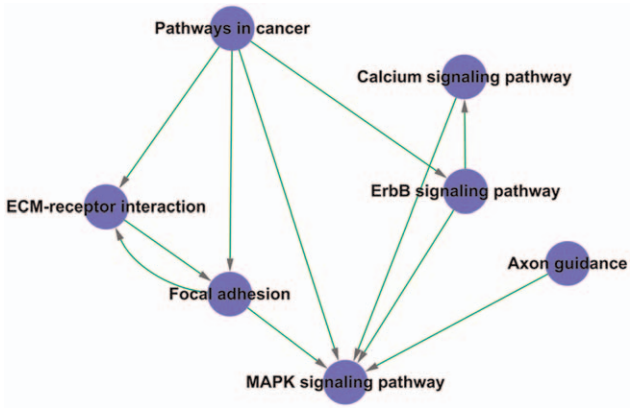

Figure 3: The interaction net of the main pathways (Pathway-net). Nodes represented pathways. The area of nodes displayed the degree that is the number of other pathways that interacted with this pathway. Lines indicate interactions between pathways, where pathways indicated by the arrowhead were regulated by pathways of the arrow tail. ECM: Extracellular matrix; MAPK: Mitogen-activated protein kinase.

increase in their expression (Col1a2, Flna: $P < 0.010$) [Figures 7–8].

Discussion

In this study, we identified several genes which were differentially expressed in both the mTLE and hip-DBS groups. The dysregulated genes are implicated in several pathways, including the calcium signaling pathway, ECM-receptor interaction, focal adhesion, and MAPK signaling pathway. These results were consistent with other high-throughput studies on mTLE in animal models and patients.[26,27] For instance, using surgically acquired hippocampi from 129 mTLE patients, Johnson *et al*[27] identified a gene-regulatory network associated with epilepsy that contains numerous highly expressed genes. The mTLE-network was significantly enriched in genes belonging to several biological pathways related to cell-to-ECM adhesion including ECM-receptor interaction and focal adhesion pathway.

Gene expression at mTLE could also be modulated by DBS. Our study revealed that there were 1062 differen-

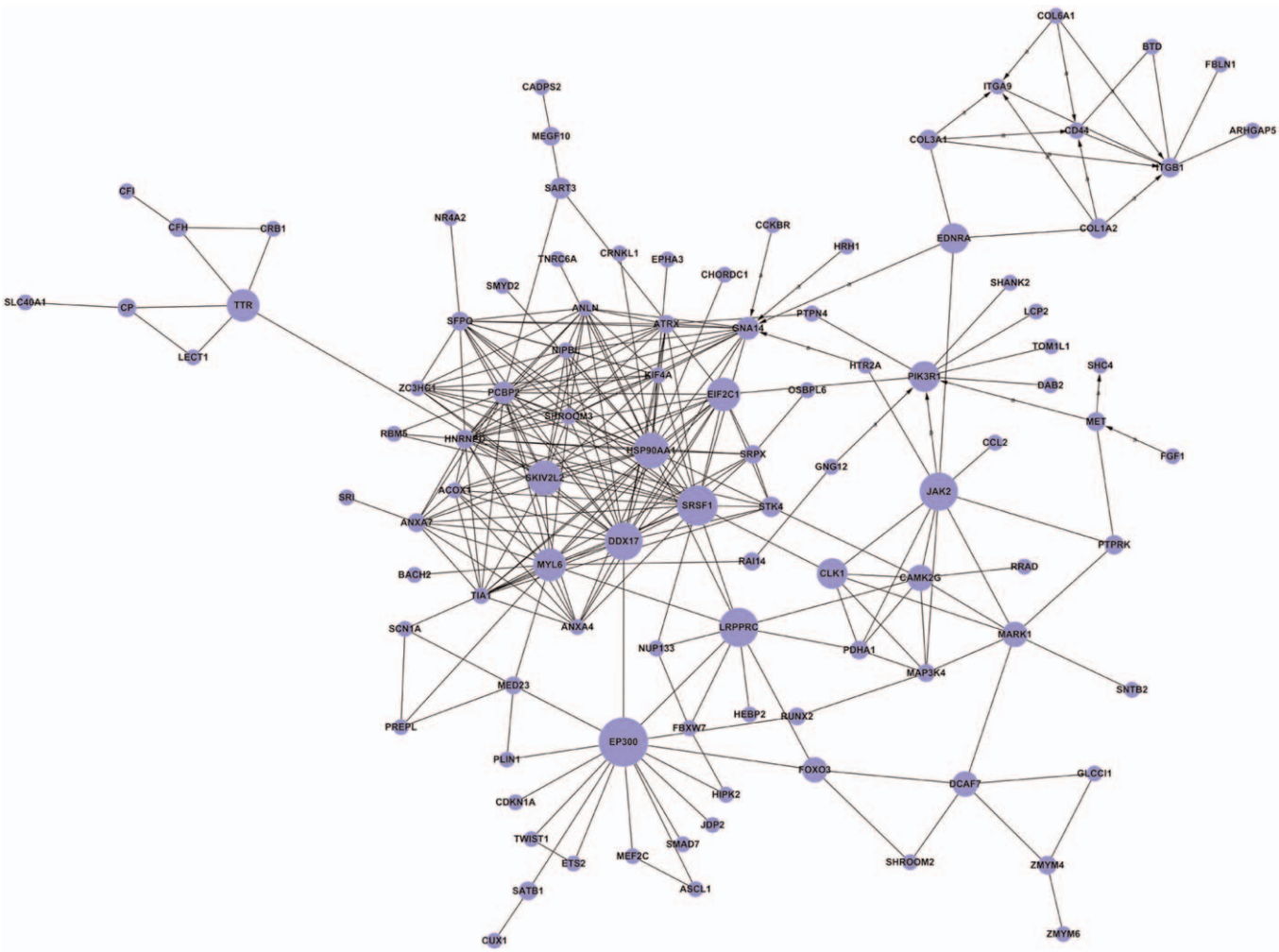

Figure 4: Signal-net analysis of all differentially expressed genes. All differential genes were connected in one network based on prior known protein-protein interactions and signaling pathways. Blue nodes represent genes. The size of nodes displayed the degree that was the number of other genes that interacted with this gene. Lines indicate interactions between genes. Directed lines denote interactions, where genes indicated by the arrowhead were regulated by genes of the arrow tail.

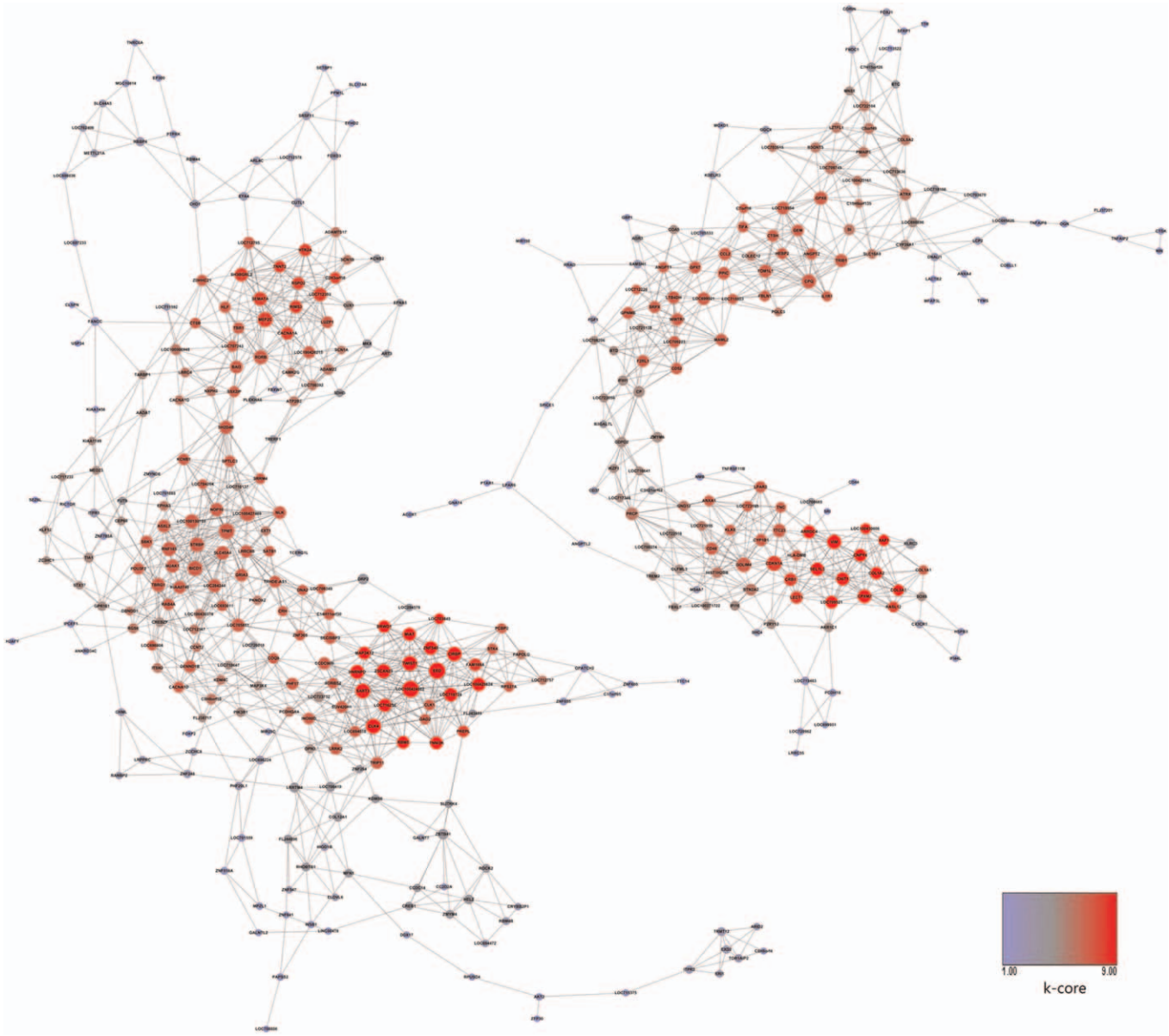

Figure 5: The global dynamic gene networks of the differentially regulated genes. The dots indicate the differentially regulated genes. The size of the dots indicates the capability of the gene to interact with others. The lines show the relationship between genes. The solid line denotes positive regulation, and the dashed line denotes negative regulation. The color of the dots indicates the regulation status of the gene, quantified by "k-core." k-core indicates the status of the evaluation of gene regulation in the network. A larger k-core for a gene indicates a larger number of interacting genes, and thus of higher importance for the gene in the network. The k-core values of the red dot were defined as 9, which means the gene had the highest regulation status in the network, while the k-core values of the blue dot were defined as 1, meaning the lowest regulation status.

tially expressed mRNAs between KA and KA + hip-DBS groups. STC analysis showed that profile 5 was the most significant profile among the 16 profiles. Genes in profile 5 were elevated in mTLE group and then gradually decreased in hip-DBS treatment group, suggesting that these genes were associated with mTLE and DBS therapy. Pathway analysis revealed that many genes in profile 5 were implicated in ECM-receptor interaction and focal adhesion pathway. To verify the accuracy of the results of microarray chips, we used qRT-PCR to validate the genes of these pathways. The results showed that six out of nine genes were in line with the expected trend, however, only one gene showed a significant difference. This may be due to the small number of rhesus monkeys in each group. To further verify the results, we selected three genes (*Col1a2*, *Itgb1*, and *Flna*) from ECM-receptor interaction and focal adhesion pathway to evaluate their expression by Western blot. We found that the expression of the three genes was increased at mTLE and all decreased under DBS. These results indicate that DBS inhibited the mTLE-caused activation of ECM-receptor interaction and focal adhesion pathways.

Focal adhesions are large sub-cellular structures through which mechanical stimulus or regulatory signals are transmitted between the ECM and an interacting cell.[28] The focal adhesion pathway is involved in several important biological processes including cell motility, cell

proliferation, cell differentiation, regulation of gene expression, and cell survival. Moreover, many focal adhesion proteins have been shown to play essential roles in epileptogenesis. It is reported that seizures could up-regulate the expression of multiple ECM and integrin molecules[29-31] including Col18a1, Lama2, metalloproteinases (MMPs), and Itgb1.[32] Moreover, patients with epilepsy with myoclonic and other types of generalized seizures were associated with *Col18a1* gene mutations,[33] and *Lama2* gene mutations were associated with focal cortical dysplasia and epilepsy.[34] Studies in mice showed that ECM molecules might shape seizure-induced mossy fibers sprouting, granule cell dispersion, and astrogliosis.[35] Tenascin R-deficient mice were resistant to epilepsy induction progression,[36] highlighting that manipulation of the ECM could have beneficial anti-epileptogenic effects. In addition, MMPs were also implicated in epileptogenesis: the sensitivity to epilepsy induction was decreased in MMP-9 knockout mice but was increased in a novel line of transgenic rats overexpressing MMP-9,[37] Furthermore, MMP-9 deficiency led to a suppression of seizure-evoked dendritic spine pruning and a decrease in aberrant synaptogenesis after mossy fiber sprouting.[37] Taken together, these findings suggest that the remodeling of focal adhesion molecules by seizures might contribute to epileptogenesis. In the current study, the focal adhesion molecules were significantly up-regulated in mTLE, which was consistent with our previous study and reports of others.[27,38] Furthermore, because DBS could modulate the dysregulation of these molecules, we selected the dysregulated genes in the ECM and focal adhesion pathways for validation. The results indicate that DBS may alleviate epilepsy by, in part, modulating the focal adhesion pathway.

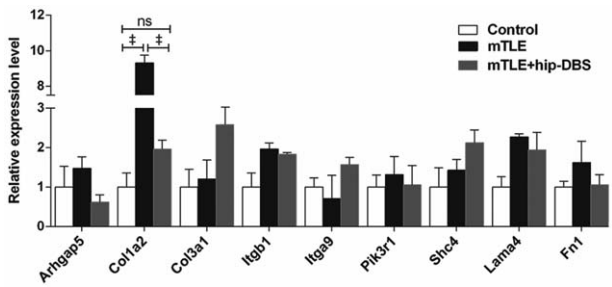

Figure 6: The differential expression genes were validated by qRT-PCR. Nine differentially expressed genes selected from profile 5 in Figure 1B were validated by qPCR. The nine genes also belong to the ECM-integrin pathway. Data were presented as mean ± SEM, $^{‡}P < 0.001$. ECM: Extracellular matrix; hip-DBS: Hippocampus -deep brain stimulation; mTLE: Medial temporal lobe epilepsy; qRT-PCR: Quantitative real-time PCR; SEM: Standard error of the mean.

In this study, we used rhesus monkey to establish a temporal lobe epilepsy model and used a Medtronic DBS system (Medtronic, Inc., Minneapolis, MN, USA) consisting of a type-3389 lead and a type-7428 internal pulse generator, which were similar to clinical application. Moreover, for the first time, we identified the molecular changes of hip-DBS on mTLE using high-throughput methods. However, because only two samples in each group were used for microarray analysis, the differentially expressed genes were screened by fold-change filtering rather than statistical analysis. Nevertheless, we believed that the microarray analysis results are reliable as the majority of the differentially expressed genes in the hippocampus of the epileptic monkeys are consistent with the findings in previous research.[38]

In summary, our findings suggest that hip-DBS could reverse mTLE-induced abnormal gene expression. Particularly, we found that hip-DBS could reverse mTLE-induced

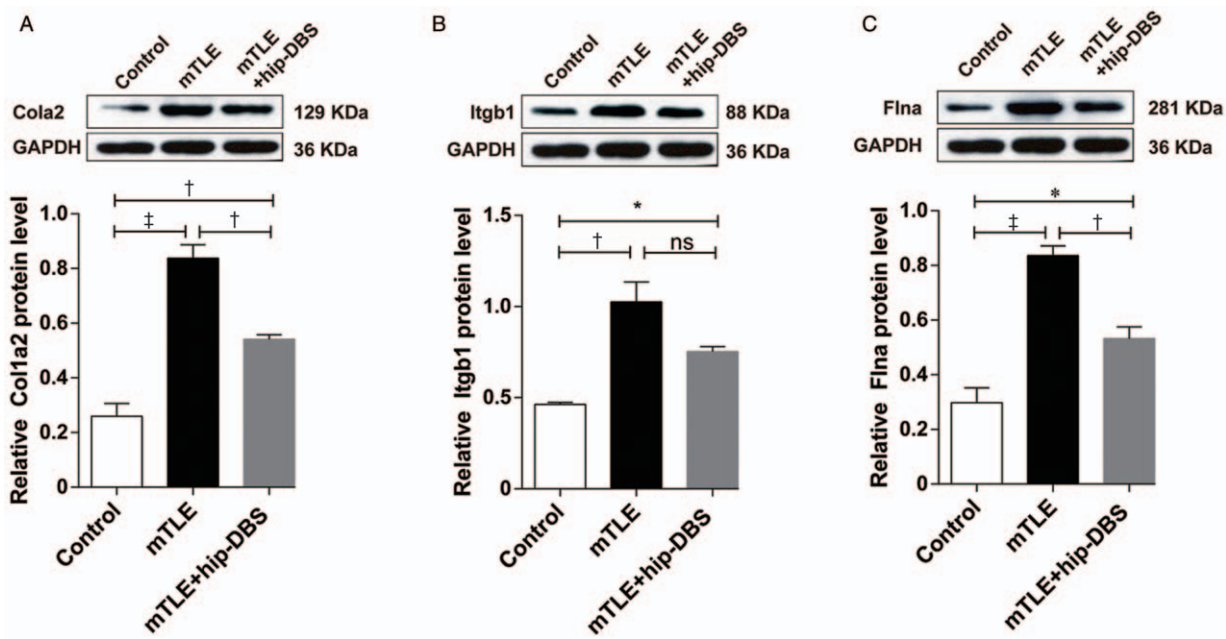

Figure 7: The differential expression genes were validated by Western blot. Three differentially expressed genes in focal adhesion pathway were further validated using Western blot ($n = 3$). The blots were densitometrically quantified, and the data were normalized to GAPDH. Data were presented as mean ± SEM, $^{*}P < 0.050$, $^{†}P < 0.010$, $^{‡}P < 0.001$. ECM: Extracellular matrix; GAPDH: Glyceraldehyde-3-phosphate dehydrogenase; hip-DBS: Hippocampus-deep brain stimulation; mTLE: Mesial temporal lobe epilepsy; SEM: Standard error of the mean.

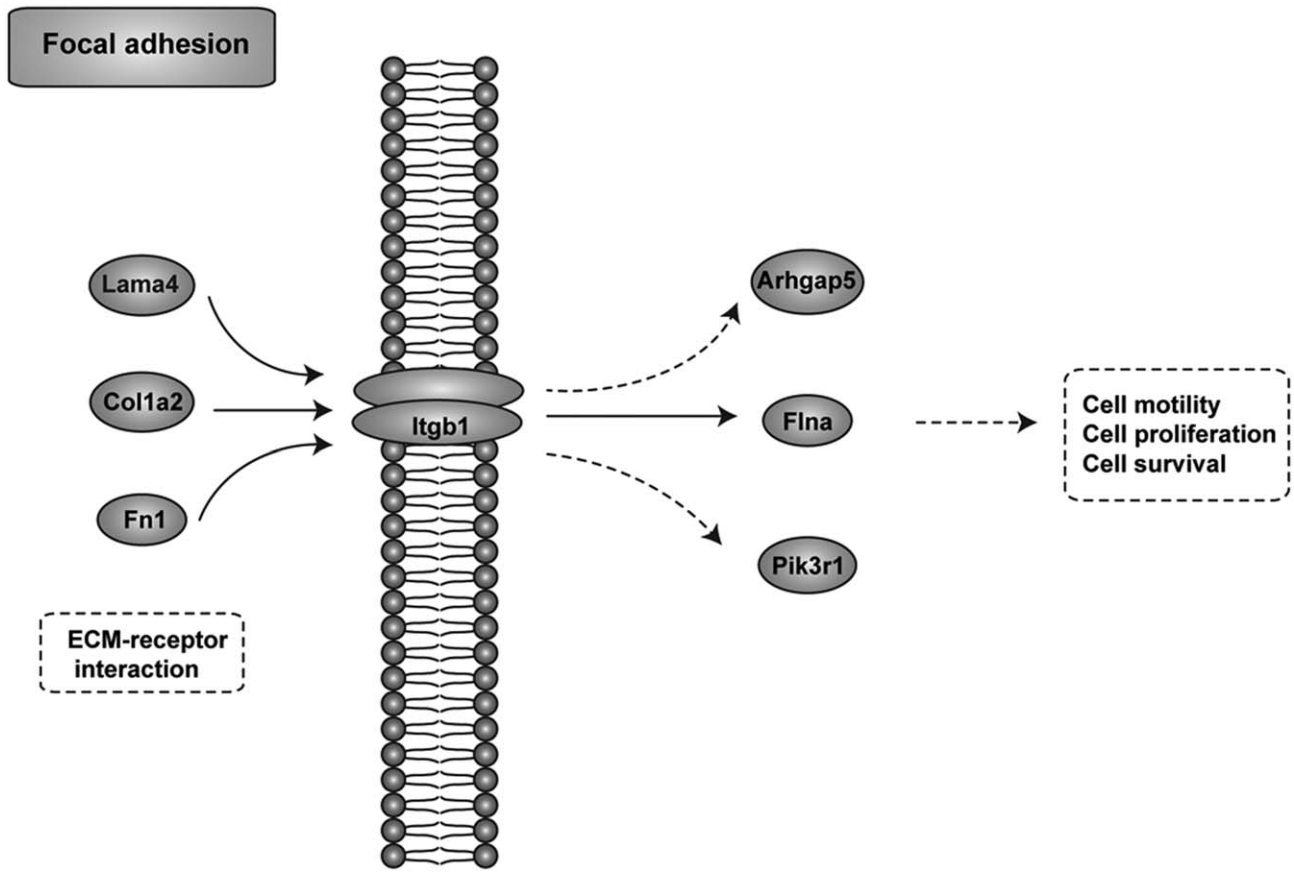

Figure 8: Schematic illustration of genes in the ECM-integrin pathway validated by qRT-PCR and Western blot. *Arhgap5*, *Col1a2*, *Itgb1*, *Pik3r1*, *Lama4*, and *Fn1* were validated by qRT-PCR; *Col1a2*, *Itgb1*, and *Flna* were validated by Western blot. Changes of all these genes were in line with the expected regulation trajectory (profile 5), that is, elevated after KA and then decreased under hip-DBS. ECM: Extracellular matrix; hip-DBS: Hippocampus-deep brain stimulation; qRT-PCR: Quantitative real-time PCR.

activation of focal adhesion pathway via antagonizing the expression increase of genes in this pathway [Figure 8]. The findings from this study provide insight in our understanding of the mechanisms underlying DBS effects for mTLE. Obviously, more studies are needed to further elucidate the molecular details involved in these events.

Funding

This study was partly supported by grants from the National Natural Science Foundation of China (Nos. 81901314, 81701251, and 81471315).

Conflicts of interest

None.

References

1. Kwan P, Schachter SC, Brodie MJ. Drug-resistant epilepsy. N Engl J Med 2011;365:919–926. doi: 10.1056/NEJMra1004418.
2. Picot MC, Baldy-Moulinier M, Daures JP, Dujols P, Crespel A. The prevalence of epilepsy and pharmacoresistant epilepsy in adults: a population-based study in a Western European country. Epilepsia 2008;49:1230–1238. doi: 10.1111/j.1528-1167.2008.01579.x.
3. Li MCH, Cook MJ. Deep brain stimulation for drug-resistant epilepsy. Epilepsia 2018;59:273–290. doi: 10.1111/epi.13964.
4. Han CL, Hu W, Stead M, Zhang T, Zhang JG, Worrell GA, *et al*. Electrical stimulation of hippocampus for the treatment of refractory temporal lobe epilepsy. Brain Res Bull 2014;109:13–21. doi: 10.1016/j.brainresbull.2014.08.007.
5. Gimenes C, Malheiros JM, Battapady H, Tannus A, Hamani C, Covolan L. The neural response to deep brain stimulation of the anterior nucleus of the thalamus: a MEMRI and c-Fos study. Brain Res Bull 2019;147:133–139. doi: 10.1016/j.brainresbull.2019.01.011.
6. Yu W, Walling I, Smith AB, Ramirez-Zamora A, Pilitsis JG, Shin DS. Deep brain stimulation of the ventral pallidum attenuates epileptiform activity and seizing behavior in pilocarpine-treated rats. Brain Stimul 2016;9:285–295. doi: 10.1016/j.brs.2015.11.006.
7. Santos-Valencia F, Almazan-Alvarado S, Rubio-Luviano A, Valdes-Cruz A, Magdaleno-Madrigal VM, Martinez-Vargas D. Temporally irregular electrical stimulation to the epileptogenic focus delays epileptogenesis in rats. Brain Stimul 2019;12:1429–1438. doi: 10.1016/j.brs.2019.07.016.
8. Ghotbedin Z, Janahmadi M, Mirnajafi-Zadeh J, Behzadi G, Semnanian S. Electrical low frequency stimulation of the kindling site preserves the electrophysiological properties of the rat hippocampal CA1 pyramidal neurons from the destructive effects of amygdala kindling: the basis for a possible promising epilepsy therapy. Brain Stimul 2013;6:515–523. doi: 10.1016/j.brs.2012.11.001.
9. Amorim BO, Covolan L, Ferreira E, Brito JG, Nunes DP, de Morais DG, *et al*. Deep brain stimulation induces antiapoptotic and anti-inflammatory effects in epileptic rats. J Neuroinflammation 2015;12:162. doi: 10.1186/s12974-015-0384-7.
10. Wu G, Hong Z, Li Y, Zhou F, Shi J. Effects of low-frequency hippocampal stimulation on gamma-amino butyric acid type B receptor expression in pharmacoresistant amygdaloid kindling epileptic rats. Neuromodulation 2013;16:105–113. doi: 10.1111/j.1525-1403.2012.00493.x.
11. Shen FZ, Wang F, Yang GM, Miao L, Wang EJ, Xu J, *et al*. The effects of low-frequency electric stimulus on hippocampal of effects of low-frequency electric stimulus on hippocampal of (alpha) 5 subunit

of extrasynapse GABAA receptor in kainic acid-induced epilepsy rats (in Chinese). Natl Med J China 2013;93:550–553. doi: 10.3760/cma.j.issn.0376-2491.2013.07.019.
12. Cuellar-Herrera M, Velasco M, Velasco F, Velasco AL, Jimenez F, Orozco S, *et al*. Evaluation of GABA system and cell damage in parahippocampus of patients with temporal lobe epilepsy showing antiepileptic effects after subacute electrical stimulation. Epilepsia 2004;45:459–466. doi: 10.1111/j.0013-9580.2004.43503.x.
13. Van Den Berge N, Keereman V, Vanhove C, Van Nieuwenhuyse B, van Mierlo P, Raedt R, *et al*. Hippocampal deep brain stimulation reduces glucose utilization in the healthy rat brain. Mol Imaging Biol 2015;17:373–383. doi: 10.1007/s11307-014-0801-9.
14. Chen N, Liu C, Yan N, Hu W, Zhang JG, Ge Y, *et al*. A macaque model of mesial temporal lobe epilepsy induced by unilateral intrahippocampal injection of kainic acid. PLoS One 2013;8:e72336. doi: 10.1371/journal.pone.0072336.
15. Chen N, Gao Y, Yan N, Liu C, Zhang JG, Xing WM, *et al*. High-frequency stimulation of the hippocampus protects against seizure activity and hippocampal neuronal apoptosis induced by kainic acid administration in macaques. Neuroscience 2014;256:370–378. doi: 10.1016/j.neuroscience.2013.10.059.
16. Xiao S, Mo D, Wang Q, Jia J, Qin L, Yu X, *et al*. Aberrant host immune response induced by highly virulent PRRSV identified by digital gene expression tag profiling. BMC Genomics 2010;11:544. doi: 10.1186/1471-2164-11-544.
17. Ashburner M, Ball CA, Blake JA, Botstein D, Butler H, Cherry JM, *et al*. Gene ontology: tool for the unification of biology. The Gene Ontology Consortium. Nat Genet 2000;25:25–29. doi: 10.1038/75556.
18. Dupuy D, Bertin N, Hidalgo CA, Venkatesan K, Tu D, Lee D, *et al*. Genome-scale analysis of in vivo spatiotemporal promoter activity in Caenorhabditis elegans. Nat Biotechnol 2007;25:663–668. doi: 10.1038/nbt1305.
19. Yi M, Horton JD, Cohen JC, Hobbs HH, Stephens RM. WholePathwayScope: a comprehensive pathway-based analysis tool for high-throughput data. BMC Bioinformatics 2006;7:30. doi: 10.1186/1471-2105-7-30.
20. Jansen R, Greenbaum D, Gerstein M. Relating whole-genome expression data with protein-protein interactions. Genome Res 2002;12:37–46. doi: 10.1101/gr.205602.
21. Li C, Li H. Network-constrained regularization and variable selection for analysis of genomic data. Bioinformatics 2008;24:1175–1182. doi: 10.1093/bioinformatics/btn081.
22. Wei Z, Li H. A Markov random field model for network-based analysis of genomic data. Bioinformatics 2007;23:1537–1544. doi: 10.1093/bioinformatics/btm129.
23. Zhang JD, Wiemann S. KEGGgraph: a graph approach to KEGG PATHWAY in R and bioconductor. Bioinformatics 2009;25:1470–1471. doi: 10.1093/bioinformatics/btp167.
24. Spirin V, Mirny LA. Protein complexes and functional modules in molecular networks. Proc Natl Acad Sci USA 2003;100:12123–12128. doi: 10.1073/pnas.2032324100.
25. Barabasi AL, Oltvai ZN. Network biology: understanding the cell's functional organization. Nat Rev Genet 2004;5:101–113. doi: 10.1038/nrg1272.
26. Dingledine R, Coulter DA, Fritsch B, Gorter JA, Lelutiu N, McNamara J, *et al*. Transcriptional profile of hippocampal dentate granule cells in four rat epilepsy models. Sci Data 2017;4:170061. doi: 10.1038/sdata.2017.61.
27. Johnson MR, Behmoaras J, Bottolo L, Krishnan ML, Pernhorst K, Santoscoy PL, *et al*. Systems genetics identifies Sestrin 3 as a regulator of a proconvulsant gene network in human epileptic hippocampus. Nat Commun 2015;6:6031. doi: 10.1038/ncomms7031.
28. Chen CS, Alonso JL, Ostuni E, Whitesides GM, Ingber DE. Cell shape provides global control of focal adhesion assembly. Biochem Biophys Res Commun 2003;307:355–361. doi: 10.1016/s0006-291x(03)01165-3.
29. Dityatev A, Fellin T. Extracellular matrix in plasticity and epileptogenesis. Neuron Glia Biol 2008;4:235–247. doi: 10.1017/S1740925X09000118.
30. Gall CM, Lynch G. Integrins, synaptic plasticity and epileptogenesis. Adv Exp Med Biol 2004;548:12–33. doi: 10.1007/978-1-4757-6376-8_2.
31. Wu X, Reddy DS. Integrins as receptor targets for neurological disorders. Pharmacol Ther 2012;134:68–81. doi: 10.1016/j.pharmthera.2011.12.008.
32. Pinkstaff JK, Lynch G, Gall CM. Localization and seizure-regulation of integrin beta 1 mRNA in adult rat brain. Brain Res Mol Brain Res 1998;55:265–276. doi: 10.1016/s0169-328x(98)00007-2.
33. Suzuki OT, Sertie AL, Der Kaloustian VM, Kok F, Carpenter M, Murray J, *et al*. Molecular analysis of collagen XVIII reveals novel mutations, presence of a third isoform, and possible genetic heterogeneity in Knobloch syndrome. Am J Hum Genet 2002;71:1320–1329. doi: 10.1086/344695.
34. Vigliano P, Dassi P, Di Blasi C, Mora M, Jarre L. LAMA2 stop-codon mutation: merosin-deficient congenital muscular dystrophy with occipital polymicrogyria, epilepsy and psychomotor regression. Eur J Paediatr Neurol 2009;13:72–76. doi: 10.1016/j.ejpn.2008.01.010.
35. Dityatev A. Remodeling of extracellular matrix and epileptogenesis. Epilepsia 2010;51 (Suppl 3):61–65. doi: 10.1111/j.1528-1167.2010.02612.x.
36. Hoffmann K, Sivukhina E, Potschka H, Schachner M, Loscher W, Dityatev A. Retarded kindling progression in mice deficient in the extracellular matrix glycoprotein tenascin-R. Epilepsia 2009;50:859–869. doi: 10.1111/j.1528-1167.2008.01774.x.
37. Wilczynski GM, Konopacki FA, Wilczek E, Lasiecka Z, Gorlewicz A, Michaluk P, *et al*. Important role of matrix metalloproteinase 9 in epileptogenesis. J Cell Biol 2008;180:1021–1035. doi: 10.1083/jcb.200708213.
38. Han CL, Zhao XM, Liu YP, Wang KL, Chen N, Hu W, *et al*. Gene expression profiling of two epilepsy models reveals the ECM/Integrin signaling pathway is involved in epiletogenesis. Neuroscience 2019;396:187–199. doi: 10.1016/j.neuroscience.2018.10.021.

How to cite this article: Chen N, Zhang JG, Han CL, Meng FG. Hippocampus chronic deep brain stimulation induces reversible transcript changes in a macaque model of mesial temporal lobe epilepsy. Chin Med J 2021;134:1845–1854. doi: 10.1097/CM9.0000000000001644